Mononuclear Lanthanide Complexes with a Long Magnetization Relaxation Time at High Temperatures: A New Category of Magnets at the Single-Molecular Level

Naoto Ishikawa,*,† Miki Sugita,† Tadahiko Ishikawa,‡ Shin-ya Koshihara,‡ and Youkoh Kaizu*,†

Departments of Chemistry and of Materials Science, Tokyo Institute of Technology, O-okayama, Meguro-ku, Tokyo 152-8551, Japan

Received: November 26, 2003; In Final Form: May 21, 2004

Alternating current (ac) magnetic susceptibility and magnetization hysteresis loop measurements have been carried out for anionic bis(phthalocyaninato)terbium and bis(phthalocyaninato)dysprosium. The two mononuclear lanthanide complexes show the characteristic temperature and frequency dependence in the ac susceptibility signals, reflecting their slow magnetization relaxation. From the Arrhenius analysis of the ac susceptibility data obtained for a diluted sample in a diamagnetic matrix, it has been found that the magnetization relaxation in the Tb complex is dominated by the two-phonon Orbach process in the temperature range 25−40 K and direct or Raman process below 25 K. In the Dy complex case, the Orbach process is the main relaxation process in the range 3−12 K. The Δ values in the Orbach term, corresponding to the height of the potential energy barrier to magnetic moment reversal, are in good agreement with the energy differences between the lowest and second lowest substates of the ground multiplet in the two cases. In the magnetization−field (**M**−**H**) loop measurements at 1.7 K, clear hysteresis has been observed for both complexes. These results indicate that the two double-decker phthalocyanine−lanthanide complexes behave as magnets at the single-molecular level. They are the first lanthanide compounds as well as the first mononuclear complexes showing such behaviors. Differences in the magnetization relaxation mechanism between the new "mononuclear lanthanide magnets" and the transition-metal-cluster-based SMMs (single-molecule magnets) are discussed.

Introduction

Understanding of dynamic magnetic properties of a high-spin molecule requires a quantitative knowledge of the sublevel structure of its ground multiplet. A recent successful example of this is the series of studies on the magnetic bistability at the single-molecular level observed for a class of transition-metal clusters known as "single-molecule magnets" (SMMs),[1] which have attracted a great deal of attention for the past decade because of their potential application to nanometer-scale memory devices. To date several types of transition-metal SMMs have been reported, including the most well studied Mn_{12} cluster derivatives $[Mn_{12}O_{12}(O_2CR)_{16}(H_2O)_x]^{n-}$ ($n = 0, 1, 2$; $x = 3, 4$),[1−5] distorted cubane complexes with $[M^{IV}M^{III}{}_4O_3X]$ cores,[6,7,8] tetranuclear vanadium complexes $[V_4O_2(O_2CR)_7(L)_2]^n$,[9] and iron complexes formulated as $[Fe_8O_2(OH)_{12}(L)_6]^{8+}$.[10]

The unusually slow magnetic relaxation and the resultant magnetic bistability of these polynuclear complexes have been explained in connection with the characteristic sublevel structures of their ground multiplets. The complexes possess a high-spin ground state with a negative axial zero-field splitting constant D, which brings the "spin-up" ($S_z = S$) and "spin-down" ($S_z = -S$) states to the lowest energy in the multiplet. Here, S is the spin angular momentum quantum number. The long magnetization relaxation time and its temperature dependence are explained by the presence of a potential barrier with a height of $U_{eff} = |D|S^2$ (S is an integer) or $U_{eff} = |D|(S^2 - 1/4)$ (S is a half-integer) between the spin-up and spin-down states. The dynamic magnetic properties of the transition-metal SMMs are thus determined essentially by the value of D, which is typically on the order of 0.1 cm^{-1} and can be determined experimentally by ESR measurements.

In contrast to those of the transition-metal complexes, the dynamic magnetic properties of lanthanide complexes have been much less explored. One of the reasons for this is that determination of multiplet sublevel structures of lanthanide complexes is generally considered difficult. In the cases in which f−f optical spectra with sufficiently narrow line widths are obtained, the substructures of the ground and excited multiplets can be directly determined through analysis of fine structures of the spectral bands. For most lanthanide complexes, however, such spectra are not available, and quantitative information about the ligand field splitting is difficult to obtain.

Recently, Ishikawa et al. reported a new approach to determination of sublevel structures of lanthanide complexes using NMR paramagnetic shifts and magnetic susceptibility data, instead of f−f optical spectroscopic ones. In this approach the set of ligand field parameters which gives the least-squares fit to the experimental data is determined under the restriction that each parameter be a linear function of the atomic number of the lanthanide.[11,12] The method has been shown to be potent to provide vital information for the study of magnetic properties of a wide range of lanthanide compounds.

We have used the approach to determine the sublevel structures of the ground multiplets of a series of multilayered phthalocyaninatolanthanide complexes, namely, Pc_2Ln^-,[13] PcLnPcYPc*, PcYPcLnPc*,[12] and PcLnPcLnPc* [14] (Pc = dianion

* To whom corresondence should be addressed. E-mail: ishikawa@chem.titech.ac.jp.
† Department of Chemistry.
‡ Department of Materials Science.

10.1021/jp0376065 CCC: $27.50
Published on Web 06/30/2004

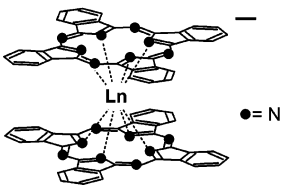

Figure 1. Schematic diagram of the anion of bis(phthalocyaninato)-lanthanide.

of phthalocyanine, Pc* = dianion of 2,3,9,10,16,17,23,24-octabutoxyphthalocyanine, Ln = Tb, Dy, Ho, Er, Tm, or Yb). In the study of Pc_2Ln^-, it was shown that Pc_2Tb^- had an especially intriguing splitting pattern of the ground multiplet: the lowest sublevel has the largest $|J_z|$ value in the $J = 6$ multiplet, where J is the total angular momentum quantum number, and the energy gap between the lowest and the next lowest sublevels is as large as a few hundred inverse centimeters. This sublevel structure of Pc_2Tb^- bears an interesting similarity to that in the transition-metal-cluster SMMs, which prompted us to study the single-molecular dynamic magnetism of the lanthanide−Pc complexes.

In a previous paper,[15] we have presented a preliminary report on the measurements of alternating current (ac) magnetic susceptibility of $[Pc_2Ln]^-TBA^+$ (Figure 1; Ln = Tb, Dy, Ho, Er, Tm, or Yb; $TBA^+ = N(C_4H_9)_4^+$). Out of the six compounds, $[Pc_2Tb]^-$ and $[Pc_2Dy]^-$ were found to show temperature and frequency dependence on ac magnetic susceptibility similar to that observed for the transition-metal SMMs, while the rest did not. These compounds are the first *lanthanide* complexes functioning as a magnet at the single-molecular level. Even more importantly, they are the first *mononuclear* metal complexes showing such properties. One of the most remarkable observations about these "mononuclear lanthanide magnets" is that the slow magnetization relaxation is observed in significantly higher temperature ranges than that of the transition-metal-cluster SMMs. The $[Pc_2Tb]^-$ and $[Pc_2Dy]^-$ complexes exhibit out-of-phase ac susceptibility χ_M'' peaks at 40 and 10 K with a 10^3 Hz ac field, respectively, while there has been no report of polynuclear transition-metal complexes with a χ_M'' peak temperature higher than 7 K.

The purposes of this paper are (i) to present detailed experimental results of ac susceptibility measurements of $[Pc_2Tb]^-TBA^+$ (**1**) and $[Pc_2Dy]^-TBA^+$ (**2**), (ii) to elucidate the mechanisms of the magnetization relaxation on the basis of analysis of the relations between magnetization relaxation time and temperature, and (iii) to report the magnetization hysteresis loop measurements for the two complexes for the first time. It will be shown that the ground multiplet sublevel structures previously determined for the complexes are the key information to understand their unique dynamic magnetism. The difference between the relaxation mechanisms in the mononuclear lanthanide magnets and the transition-metal cluster SMMs, for which the "double-well-potential" model applies, is discussed.

Experiments

The powder samples of **1** and **2** as well as $[Pc_2Ln]^-TBA^+$ (Ln = Ho, Er, Tm, or Yb) were prepared by the literature method[16,17] with minor modifications. Purifications were carried out by column chromatography on silica gel with careful attention given to the potential contaminant of noncharged $[Pc_2Ln]^0$. Dilution of **1** or **2** in a diamagnetic $[Pc_2Y]^-TBA^+$ matrix was carried out by recrystallization from a chloroform−hexane solution of the mixture of the two compounds in a designated molar ratio. The ac magnetic susceptibility and hysteresis loop measurements were carried out on a Quantum Design MPMS-XL magnetometer. All the microcrystalline powder samples were dispersed in either eicosane or Apiezon N grease to prevent potential torquing of the magnetically anisotropic samples.

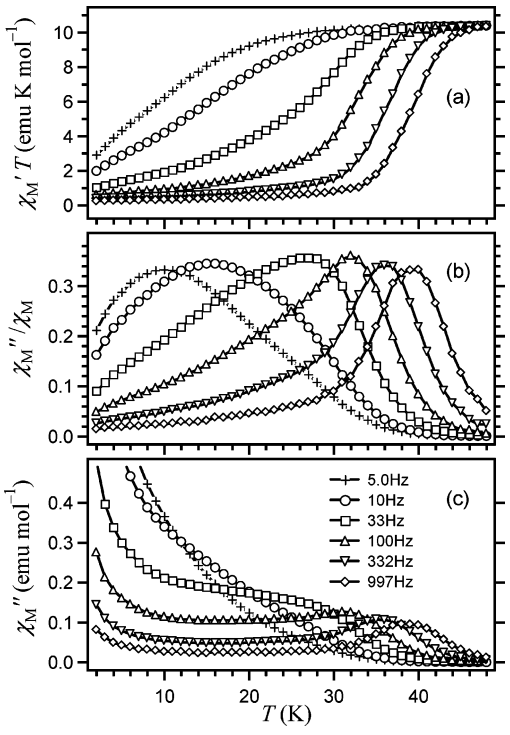

Figure 2. (a) $\chi_M'T$, (b) χ_M''/χ_M, and (c) χ_M'' against temperature T, where χ_M', χ_M'', and χ_M are in-phase ac, out-of-phase ac, and dc molar magnetic susceptibilities, respectively, for a powder sample of **1** measured in zero dc magnetic field with a 3.5 G ac field oscillating at the indicated frequencies.

Results and Discussion

Figure 2 shows the results of the ac magnetic susceptibility measurements for the microcrystalline powder of **1** with varied ac magnetic field frequencies. The top, middle, and bottom panels present $\chi_M'T$, χ_M''/χ_M, and χ_M'' values as a function of temperature T, respectively, where χ_M' and χ_M'' are in-phase and out-of-phase components of the ac molar susceptibility and χ_M is the dc molar susceptibility. The dc susceptibility measurements of **1** and the other isostructural compounds of Dy, Ho, Er, Tm, and Yb have been reported in a previous paper.[13]

As shown in the top panel, the $\chi_M'T$ values for all the ac frequencies below 1000 Hz converge at 48 K to the value corresponding to the dc χ_MT value. Each $\chi_M'T$ vs T plot exhibits a sudden decrease with decreasing T in the temperature range depending on the ac frequency, indicating that the response of the magnetic moment to the alternating magnetic field is becoming slower. The χ_M''/χ_M vs T plots in the middle panel show a peak at the temperature range where the $\chi_M'T$ dispersion curve is observed. At each χ_M''/χ_M peak temperature, the magnetization relaxation time τ of the sample matches the inverse of the angular frequency ω of the applied ac magnetic field.[18]

This magnetic relaxation behavior is similar to that observed for the transition-metal SMMs. To ensure that the slow magnetization relaxation is an intrinsic molecular property, the measurement was carried out for a diluted sample of **1** in a diamagnetic matrix.

Figure 3 shows the ac magnetic susceptibility data for **1** in the $[Pc_2Y]^-TBA^+$ matrix with the molar ratio $[Pc_2Tb]^-/[Pc_2Y]^-$

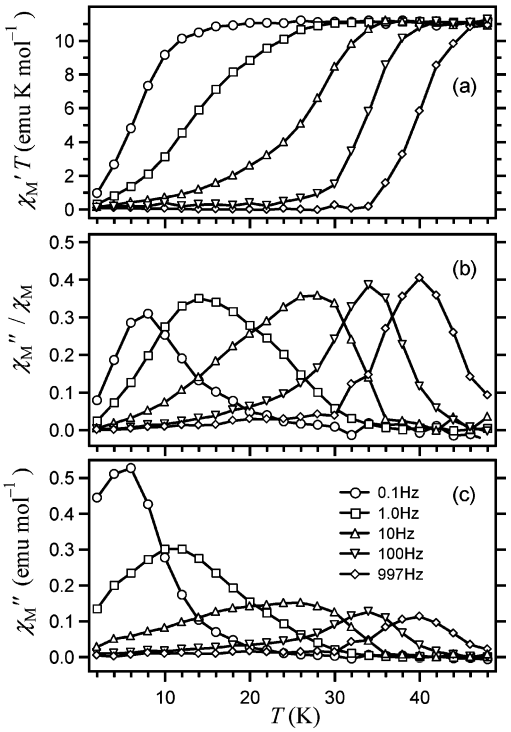

Figure 3. (a) $\chi_M'T$, (b) χ_M''/χ_M, and (c) χ_M'' against temperature T for a powder sample of **1** diluted in $[Pc_2Y]^-TBA^+$ with the ratio [Tb]/[Y] = 1/50, measured in zero dc magnetic field with a 3.5 G ac field oscillating at the indicated frequencies. The lines are visual guides.

= 1/50 at ac frequencies of 0.1, 1.0, 10, 100, and 997 Hz. The peaks of χ_M''/χ_M plots of 10, 100, and 997 Hz shifted to higher temperature or remained unchanged (28, 34, and 40 K, respectively) compared to those of the undiluted sample (16, 32, and 40 K). This indicates that the intermolecular interactions between adjacent $[Pc_2Tb]^-$ complexes shorten the relaxation time in the lower temperature range. The experiments clearly show that the slow magnetization relaxation is an intrinsic single-molecular property of $[Pc_2Tb]^-$, rather than resulting from intermolecular interactions and long-range order.

All the χ_M'' vs T plots in Figure 3c show a clear peak even with an ac field frequency of 0.1 Hz. In contrast, the undiluted sample (Figure 2c) exhibits no χ_M'' peak for an ac frequency of 33 Hz and below, and shows an increase of the χ_M'' value at low temperature with all the frequencies. This is also ascribed to the magnetic interactions between adjacent Tb complexes.

Similar magnetic relaxation behavior is observed for dysprosium complex **2**. Figure 4 shows the temperature dependence of the ac susceptibility of the undiluted sample of **2** measured at ac frequencies of 5, 10, 33, 100, 332, and 997 Hz. The $\chi_M'T$ values for all the ac frequencies converge at 23 K to the value of the dc χ_MT (top panel). Each $\chi_M'T$ plot shows a characteristic decrease with decreasing T in the temperature range depending on the applied ac field frequency. In each temperature range where a $\chi_M'T$ drop is observed, the corresponding χ_M''/χ_M vs T plot exhibits a peak.

A dilute sample of **2** in $[Pc_2Y]^-TBA^+$ (molar ratio $[Pc_2Dy]^-/[Pc_2Y]^- = 1/50$) also exhibits frequency-dependent ac susceptibilities (Figure 5). The peaks of χ_M''/χ_M vs T plots shift to higher temperature by dilution but with a much smaller degree than in the Tb case: the undiluted sample gives peaks at 4.5, 7, and 11.5 K, while the diluted sample gives peaks at 5.5, 7.5, and 12 K with ac frequencies of 10, 100, and 997 Hz, respectively. The amplitudes of the molar susceptibilities are essentially unchanged in the diluted sample. These results

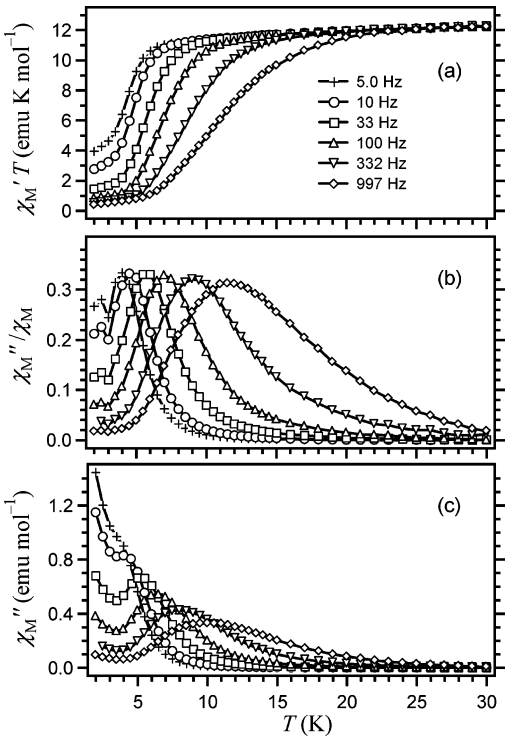

Figure 4. (a) $\chi_M'T$, (b) χ_M''/χ_M, and (c) χ_M'' against temperature T, where χ_M', χ_M'', and χ_M are in-phase ac, out-of-phase ac, and dc molar magnetic susceptibilities, respectively, for a powder sample of **2** measured in zero dc magnetic field with a 3.5 G ac field oscillating at the indicated frequencies.

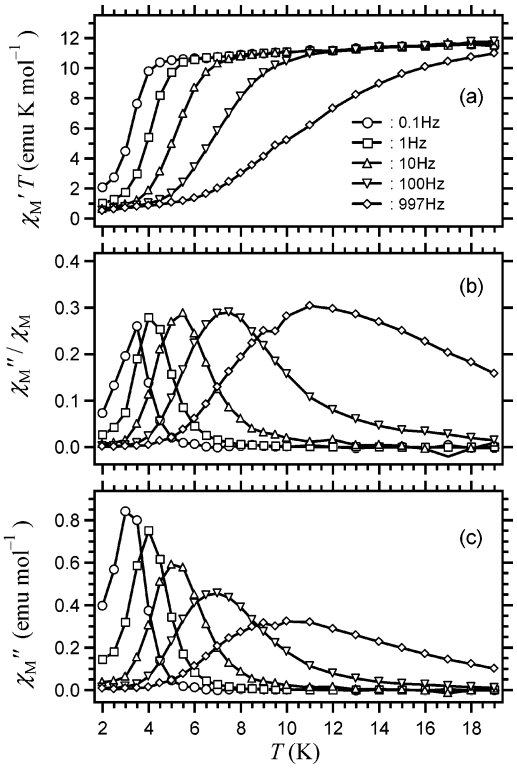

Figure 5. (a) $\chi_M'T$, (b) χ_M''/χ_M, and (c) χ_M'' against temperature T for a powder sample of **2** diluted in $[Pc_2Y]^-TBA^+$ with the ratio [Dy]/[Y] = 1/50, measured in zero dc magnetic field with a 3.5 G ac field oscillating at the indicated frequencies. The lines are visual guides.

indicate that the slow relaxation in Dy complex **2** is an intrinsic single-molecular property as in the above Tb complex case.

The effect of dilution is also seen in the low-temperature range. All the χ_M'' vs T plots of the undiluted sample show an

increase as the temperature approaches 2 K (Figure 4c), whereas the χ_M'' values of the diluted sample decrease or stay at the zero level (Figure 5c). In addition, while the χ_M'' peak becomes unclear at a 5 Hz ac field in the undiluted case, a clear peak is seen in all the χ_M'' plots with all the frequencies down to 0.1 Hz in the diluted case. These observations are attributable to the presence and absence of the intermolecular magnetic interactions between adjacent Dy complexes.

In the field of transition-metal SMMs, the magnetization relaxation phenomena observed in the ac susceptibility measurements are recognized as the moment reversal occurring via the thermally activated process described by the equation $\tau^{-1} = \tau_0^{-1} \exp(-U_{eff}/kT)$, where U_{eff} is the height of the potential-energy barrier between the two states with $S_z = \pm S$. The barrier height is related to the zero-field splitting constant D by the equation $U_{eff} = DS^2$. An additional shortcut path is established when the energies of the sublevels with different $|S_z|$ values coincide by Zeeman interaction under an appropriate external magnetic field ("resonant tunneling process"). Under a zero dc field, the transition from the spin-up ($S_z = S$) to spin-down ($S_z = -S$) state requires climbing up to the highest sublevel with $S_z = 0$ (or 1/2). In this double-well-potential model, the number of phonons or steps involved in the thermally activated process is not explicitly defined. To our knowledge, it has not been determined whether the climbing-up process consists of multistep transitions to the intervening sublevels with $|S| < S_z < 0$ (or 1/2) or a direct transition to the highest sublevel.

On the other hand, the relaxation processes of lanthanide ions in crystalline environments have been understood in a rather different way. The relaxation mechanism is formulated as the energy exchange processes between the paramagnetic ions and phonon radiation, which are induced by the modulation of the crystal or ligand field under the action of the lattice vibrations.[19,20] The crystal or ligand field potential V is expanded with the powers of the fluctuating strain ϵ caused by the lattice vibrations:

$$V = V^{(0)} + \epsilon V^{(1)} + \epsilon^2 V^{(2)} + ...$$

where $V^{(0)}$ is the static potential. There are three major processes to be considered for the transition between the lowest two substates: (1) the direct process,[21,22] in which a phonon of the same energy as the energy difference ($h\nu$) between the spin-up and spin-down states, which are split by either the Zeeman interaction or the ligand-field potential or both, is absorbed or emitted by the spin system; (2) the Raman process,[21] where a phonon of any energy ($h\nu_p$) is scattered by the spin system as a phonon with an energy of $h\nu_p + h\nu$ or $h\nu_p - h\nu$; (3) the Orbach process,[23] involving a phonon absorption by a direct process to excite the spin system to a higher state at an energy Δ above the lowest sublevels, followed by the emission of another phonon with an energy of $\Delta + h\nu$ or $\Delta - h\nu$.

For non-Kramers systems, which contain even numbers of electrons as in a Tb^{3+} ion with a $(4f)^8$ configuration, the relaxation time obeys the following equation:[19]

$$\tau^{-1} = R_d(h\nu)^3 \coth(h\nu/2kT) + R_{or}\Delta^3\{\exp(\Delta/kT) - 1\}^{-1} + R_r T^7 \quad (1)$$

Here, the three terms on the right-hand side represent the direct, Orbach, and Raman processes, respectively. The parameter R_d is proportional to the square of the matrix element of $V^{(1)}$ between the initial state $|a\rangle$ and the final state $|b\rangle$, and R_{or} to the product of matrix elements of $V^{(1)}$ between $|a\rangle$ and $|b\rangle$ and the intermediate excited state $|c\rangle$. The third term consists of first- and second-order Raman contributions. The former contains matrix elements of $V^{(2)}$ between $|a\rangle$ and $|b\rangle$, and the latter the product of matrix elements of $V^{(1)}$ between $|a\rangle$ and $|b\rangle$ and a virtual state, $|c\rangle$.

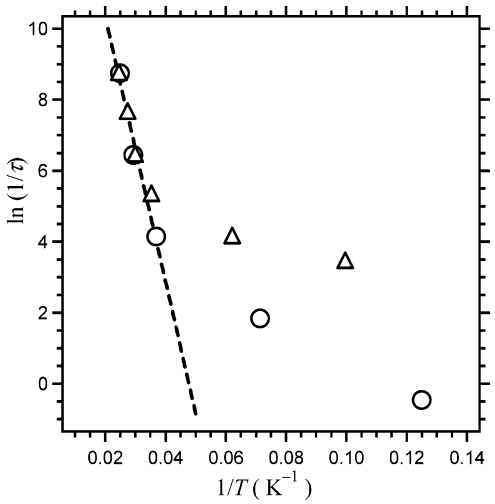

Figure 6. Natural logarithm of the magnetization relaxation rate against the inverse of the temperature of the peak of the χ_M''/χ_M value for the undiluted powder sample of **1** $[Pc_2Tb]^-TBA^+$ (triangles) and that diluted at 1:50 in $[Pc_2Y]^-TBA^+$ (circles).

When $h\nu \ll kT$, as in the present conditions for the ac measurements, the first term can be approximated by $R_d(h\nu)^2(2kT)$, giving the term linear in T. In the range where $h\nu \ll kT \ll \Delta$, the Orbach term is approximated by $R_{or}\Delta^3 \exp(-\Delta/kT)$, which indicates a thermally activated character of this process. The point that should be noted here is that this formalism does not use the double-well-potential picture.

If the Orbach process is dominant, it is possible to estimate the value of Δ, which is closely related to the "barrier height" U_{eff} in the double-well-potential picture, by the Arrhenius analysis of the magnetization relaxation time τ and temperature T. Figure 6 shows the plots of $\ln(\tau^{-1})$ vs $1/T$ for undiluted and diluted samples of **1**, where T is the χ_M''/χ_M peak temperature at which τ^{-1} matches the angular frequency ω of the applied ac field. As seen in the figure, each plot is divided into two parts. The data points in the higher temperature (higher frequency) parts of both the diluted and undiluted cases fit a single straight line. The linear relation of $\ln(\tau^{-1})$ to $1/T$ indicates that the Orbach process is dominant in the higher temperature range. From the data points for the diluted sample measured with ac frequencies from 997 to 10 Hz, the value of Δ is estimated to be 2.6×10^2 cm^{-1} with a preexponential factor (τ_0^{-1}) of 5.0×10^7 s^{-1}. The value of Δ represents the energy of the substate through which the two-phonon relaxation process occurs.

In contrast to those in the higher temperature part, the data points in the lower-temperature parts are shifted to longer relaxation time by the dilution, meaning that a relaxation process enhanced by the spin−spin interaction between adjacent Tb complexes becomes dominant in the undiluted sample in this temperature range. The data points in the lower temperature part do not fit the above-mentioned straight line for the Orbach process after the dilution to such a concentration that intermolecular spin−spin interactions can be ignored (2%). This indicates that either the direct or Raman process is dominant in the temperature range below about 25 K.

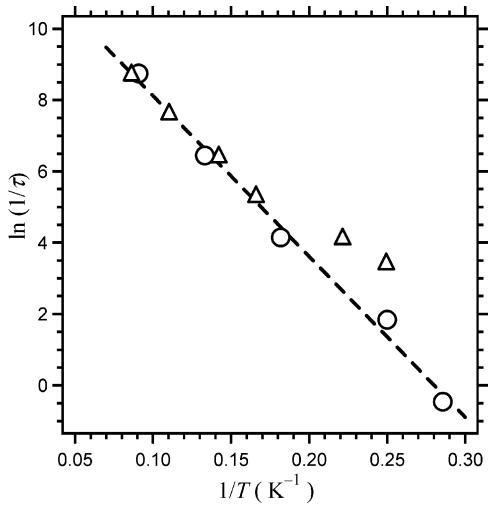

Figure 7. Natural logarithm of the magnetization relaxation rate against the inverse of the temperature of the peak of the χ_M''/χ_M value for the undiluted powder sample of **2** $[Pc_2Dy]^-TBA^+$ (triangles) and that diluted at 1:50 in $[Pc_2Y]^-TBA^+$ (circles).

For Kramers systems containing odd numbers of electrons the relaxation time is formulated as[19]

$$\tau^{-1} = R_d(h\nu)^5 \coth(h\nu/2kT) + R_{or}\Delta^3\{\exp(\Delta/kT) - 1\}^{-1} + R_rT^9 + R_r'(h\nu/k)^5T^7 \quad (2)$$

As in the above non-Kramers case, the second term is approximated as $R_{or}\Delta^3 \exp(-\Delta/kT)$ in the range $h\nu \ll kT \ll \Delta$. The Arrhenius plots for the undiluted and diluted samples of the Dy complex **2** with a $(4f)^9$ configuration are shown in Figure 7. All the data points for the diluted sample lie along a single straight line. This indicates that the Orbach process is again dominant but in the entire temperature range from 12 down to 3 K. The undiluted sample shows a departure from linearity in the low-temperature range. This is interpreted as the effect of the intermolecular spin−spin interaction as in the above Tb case. From the data for the diluted sample, the value of Δ is estimated to be 3.1×10^1 cm^{-1} with a preexponential factor (τ_0^{-1}) of 3.0×10^5 s^{-1}. The value of Δ is greatly reduced from that of the Tb complex case, indicating that the energy of the substate through which the two-phonon relaxation process occurs is much lower than that in the Tb case.

In both Tb and Dy cases, the Arrhenius analysis suggests that the main relaxation path in the higher temperature range is the Orbach process. This conclusion is strongly supported by the previously determined sublevel structures of the ground multiplets of these complexes. Figure 8 shows the substate energy levels of the six lanthanide complexes for which we have carried out the ac susceptibility measurements.[13] The values of Δ for the Tb and Dy complexes (2.6×10^2 and 3.1×10^1 cm^{-1}, respectively) are in good agreement with the energy separations between the first and second lowest sublevels (about 400 and 40 cm^{-1}, respectively). This strongly supports the assignment to the Orbach process, and also that the process occurs through the second lowest substate. The difference between the Tb and Dy cases in the temperature dependences of the magnetic relaxation phenomena is thus explained by the difference in the energies of the second lowest sublevels.

Figure 8 also gives information about the reason the slow magnetization relaxation is observed for the Tb and Dy complexes but not for the other four cases. In Tb complex **1**, the lowest substates are assigned to $J_z = \pm 6$, which are the

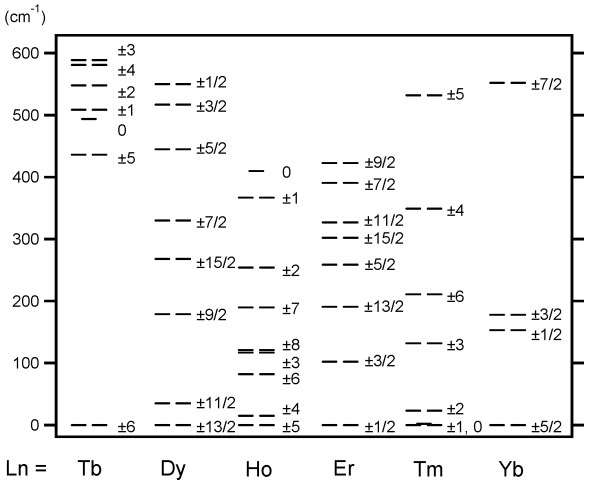

Figure 8. Energy diagram of the substates of the ground multiplets of $[Pc_2Ln]^-TBA^+$ (Ln = Tb, Dy, Ho, Er, Tm, or Tb) determined in ref 13. The J_z value of each substate is indicated to the right of the corresponding energy level.

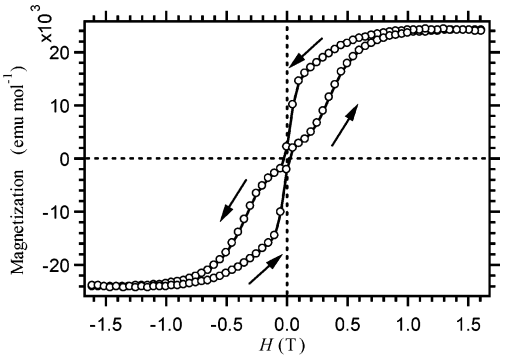

Figure 9. Magnetization vs field plot measured at 1.7 K for a powder sample of **1** $[Pc_2Tb]^-TBA^+$ diluted at a concentration of 2% in $[Pc_2Y]^-TBA^+$. The lines are visual guides.

maximum and minimum values in the $J = 6$ ground multiplet. In Dy complex **2**, the lowest substates are characterized as $J_z = \pm 13/2$, the second largest in the $J = 15/2$ ground state. In Er, Tm, and Yb cases, the absolute values of J_z are much smaller than in the Tb and Dy cases. The smaller $|J_z|$ results in greater matrix elements of $V^{(1)}$ or $V^{(2)}$ appearing in eq 1 or 2, leading to greater relaxation rates. In the Ho case, the $|J_z|$ value is not significantly different from that of the Tb case, but the energy of the second lowest substate is much lower, resulting in a faster relaxation by the Orbach process.

Magnetic bistability of a transition-metal cluster SMM can manifest itself as a magnetization hysteresis[1−3] in addition to the magnetization relaxation effect observed in an ac susceptibility measurement. To see if this is also the case for the present mononuclear lanthanide complex cases, we measured magnetization hysteresis data for **1** and **2**. Figure 9 shows the magnetization vs magnetic field (**M**−**H**) plot for Tb complex **1** diluted in the diamagnetic matrix.

The sample was cooled to 1.7 K in zero field, and then the magnetic field was increased to 1.6 T, at which the magnetization was saturated (2.4×10^4 emu mol^{-1}). The magnetization was then measured while the field was swept from +1.6 to −1.6 T and back. Each measurement point took 5−10 s, and the entire hysteresis loop took 40 min to measure. As shown in the figure, a clear hysteresis behavior is observed: the value of the magnetization in the descending path from $\mathbf{H} = 1.6$ T to $\mathbf{H} = 0$ T is greater than the corresponding value in the ascending path from $\mathbf{H} = 0$ T to $\mathbf{H} = 1.6$ T. In the region $|\mathbf{H}| > 0.1$ T,

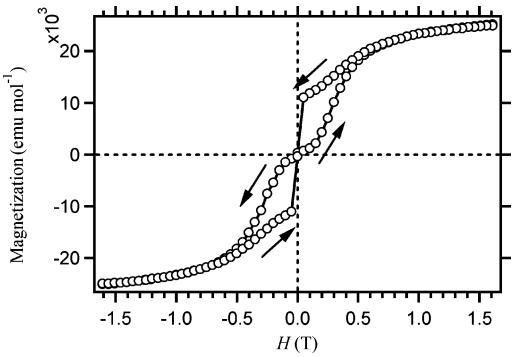

Figure 10. Magnetization vs field plot measured at 1.7 K for a powder sample of **2** $[Pc_2Dy]^-TBA^+$ diluted at a concentration of 2% in $[Pc_2Y]^-TBA^+$. The lines are visual guides.

the decrease of the values of magnetization in the descending path is relatively small. In contrast, the magnetization value drops sharply with decreasing $|\mathbf{H}|$ in the region $|\mathbf{H}| < 0.1$ T. This indicates that the relaxation time for the lower $|\mathbf{H}|$ region is relatively shorter than that for the higher $|\mathbf{H}|$ region. The value of magnetization at $\mathbf{H} = 0$ T in this experimental condition was 2.1×10^3 emu mol^{-1}.

The result of the **M**−**H** curve measurement for Dy complex **2** at 1.7 K is shown in Figure 10. The experimental conditions for the sweep time, **H** increment, and number of data points were the same as in the above Tb complex case.

The figure shows that **2** also exhibits a clear hysteresis loop. The shape of the loop resembles that of **1**, but there are a few noticeable differences from the Tb case. First, the magnetization value for the ascending path and that for the descending path meet at $|\mathbf{H}| = 0.7$ T and take the same values in the region $|\mathbf{H}| > 0.7$ T even though the magnetization is not saturated. Second, the drop in magnetization starts from the lower $|\mathbf{H}|$ value. The magnetization value at $\mathbf{H} = 0$ T is 3×10^2 emu mol^{-1}, which is 1 order smaller than that of **1**. This reflects the shorter relaxation time of **2**.

It is known that **M**−**H** loops of transition-metal-cluster SMMs show the characteristic step structures which are caused by the "resonant tunneling" process. Relaxation through this path occurs when the energy of the lowest substate with $S_z = S$ (or $-S$) coincides with one of the excited states with $S_z = -S + n$ (or $S - n$), $n = 1, 2, ...$, by the Zeeman interaction. In the present lanthanide complex cases, this energy-level crossing does not occur under the magnetic field used in this experiment, because of the large energy difference between the lowest and second lowest substates. For this reason, no step structure is observed in the **M**−**H** loops.

Conclusions

We have shown that mononuclear lanthanide complexes **1** and **2** exhibit magnetization hysteresis loops and the temperature and frequency dependence of the ac magnetic susceptibility typical of magnets at the single-molecular level. From the analysis of the temperature dependence of magnetization relaxation time, the following conclusions have been drawn regarding the relaxation processes of the two cases. In Tb complex **1**, the two-phonon Orbach process is dominant in the temperature range 25−40 K, and either the direct or Raman process becomes the fastest path below 25 K. In Dy complex **2**, the Orbach process is the main path in the range 3−12 K. The energies of the excited sublevels through which the Orbach process occurs have been estimated to be 2.6×10^2 and 3.1×10^1 cm^{-1} for the Tb and Dy complexes, respectively. The good agreement of these values with the previously determined energy differences between the lowest and the second lowest sublevels strongly supports the dominance of the Orbach process in **1** and **2**. We emphasize here that the determination of the sublevel structure of these lanthanide complexes enabled us to understand their dynamic magnetism.

The slow magnetization relaxation at the single-molecular level of **1** and **2** results from a mechanism different from that of the transition-metal-cluster SMMs. In the mononuclear lanthanide magnets, the origin of the magnetism is both orbital and spin angular momenta of a single ion, while that of the transition-metal SMMs is the spin angular momenta of multiple magnetic ions. The long magnetization relaxation times of the Tb and Dy ions in **1** and **2** are caused by the ligand field potential that brings the substates with a large $|J_z|$ value to the lowest energy level, whereas those of the transition-metal SMMs are caused by the magnetic interactions between component metal ions, leading to a negative zero-field splitting constant.

Acknowledgment. This work was partially supported by Grant-in-Aid for Science Research No. 15550046 and by the COE21 Program from the Ministry of Education, Science Sports and Culture of Japan.

References and Notes

(1) (a) Sessoli, R.; Tsai, H.-L.; Schake, A. R.; Wang, S.; Vincent, J. B.; Folting, K.; Gatteschi, D.; Christou, G.; Hendrickson, D. N. *J. Am. Chem. Soc.* **1993**, *115*, 1804. (b) Sessoli, R.; Gatteschi, D.; Caneschi, A.; Novak, M. A. *Nature* **1993**, *365*, 141.

(2) (a) Thomas, L.; Lionti, F.; Ballou, R.; Gatteschi, D.; Sessoli, R.; Barbara, B. *Nature* **1996**, *383*, 145. (b) Friedman, J. R.; Sarachik, M. P. *Phys. Rev. Lett.* **1996**, *76*, 3830.

(3) (a) Eppley, H. J.; Tsai, H.-L.; de Vries, N.; Folting, K.; Christou, G.; Hendrickson, D. N. *J. Am. Chem. Soc.* **1995**, *117*, 301. (b) Aubin, S. M. J.; Spagna, S.; Eppley, H. J.; Sager, R. E.; Christou, G.; Hendrickson, D. N. *Chem. Commun.* **1998**, 803. (c) Aubin, S. M. J.; Sun, Z.; Pardi, L.; Krzystek, J.; Folting, K.; Brunel, L.-C.; Rheingold, A. L.; Christou, G.; Hendrickson, D. N. *Inorg. Chem.* **1999**, *38*, 5329.

(4) Soler, M.; Chandra, S. K.; Ruiz, D.; Davidson, E. R.; Hendrickson, D. N.; Christou, G. *Chem. Commun.* **2000**, 2417.

(5) Boskovic, C.; Pink, M.; Huffman, J. C.; Hendrickson, D. N.; Christou, G. *J. Am. Chem. Soc.* **2001**, *123*, 9914.

(6) Aubin, S. M. J.; Wemple, M. W.; Adams, D. M.; Tsai, H.-L.; Christou, G.; Hendrickson, D. N. *J. Am. Chem. Soc.* **1996**, *118*, 7746.

(7) (a) Aubin, S. M. J.; Dilley, N. R.; Pardi, L.; Krzystek, J.; Wemple, M. W.; Brunel, L. C.; Maple, M. B.; Christou, G.; Hendrickson, D. N. *J. Am. Chem. Soc.* **1998**, *120*, 4991. (b) Andres, H.; Basler, R.; Gudel, H.-U.; Aromi, G.; Christou, G.; Buttner, H.; Ruffle, B. *J. Am. Chem. Soc.* **2000**, *122*, 12469.

(8) Andres, H.; Basler, R.; Gudel, H.-U.; Aromi, G.; Christou, G.; Buttner, H.; Ruffle, B. *J. Am. Chem. Soc.* **2000**, *122*, 12469.

(9) Castro, S. L.; Sun, Z.; Grant, C. M.; Bollinger, J. C.; Hendrickson, D. N.; Christou, G. *J. Am. Chem. Soc.* **1998**, *120*, 2997.

(10) Sangregorio, C.; Ohm, T.; Paulsen, C.; Sessoli, R.; Gatteschi, D. *Phys. Rev. Lett.* **1997**, *78*, 4645.

(11) Ishikawa, N. *J. Phys. Chem. A* **2003**, *107*, 5831.

(12) Ishikawa, N.; Iino, T.; Kaizu, Y. *J. Phys. Chem. A* **2002**, *106*, 9543.

(13) Ishikawa, N.; Sugita, M.; Okubo, T.; Tanaka, N.; Iino, T.; Kaizu, Y. *Inorg. Chem.* **2003**, *42*, 2440.

(14) (a) Ishikawa, N.; Iino, T.; Kaizu, Y. *J. Am. Chem. Soc.* **2002**, *124*, 11440. (b) Ishikawa, N.; Iino, T.; Kaizu, Y. *J. Phys. Chem. A* **2003**, *107*, 7879.

(15) Ishikawa, N.; Sugita, M.; Ishikawa, T.; Koshihara, S.; Kaizu, Y. *J. Am. Chem. Soc.* **2003**, *125*, 8694.

(16) De Cian, A.; Moussavi, M.; Fischer, J.; Weiss, R. *Inorg. Chem.* **1985**, *24*, 3162.

(17) Konami, H.; Hatano, M.; Tajiri, A. *Chem. Phys. Lett.* **1989**, *160*, 163.

(18) The Bloch equation for the longitudinal magnetization, $d\mathbf{M}(t)/dt = (1/\tau)(\chi_M\mathbf{H}(t) - \mathbf{M}(t))$, gives $\chi_M'' = \omega\tau\chi_M/(1 + \omega^2\tau^2)$, where τ is the magnetization relaxation time and ω is the angular frequency of the applied ac magnetic field $\mathbf{H}(t)$. When χ_M is a function of T, τ becomes equal to $1/\omega$ at a χ_M''/χ_M peak temperature which corresponds to the condition $d(\chi_M''/\chi_M)/dT = 0$, but does not at a χ_M'' peak temperature where $d\chi_M''/dT = 0$. We use the χ_M''/χ_M peaks in the present paper because of the wide temperature range to be considered, where χ_M greatly varies. In contrast,

the χ_M'' peak, which is commonly used in the field of SMMs, gives an approximate value for the temperature at which τ matches $1/\omega$.

(19) Abragam, A.; Bleaney, B. *Electron Paramagnetic Resonance*; Clarendon Press: Oxford, 1970; Chapter 10.

(20) Poole, C. P., Jr.; Farach, H. A. *Handbook of Electron Spin Resonance*; AIP Press: New York, 1993; Chapter 4.

(21) (a) Van Vleck, J. H. *Phys. Rev.* **1940**, *57*, 426. (b) Van Vleck, J. H. *J. Chem. Phys.* **1939**, *7*, 72.

(22) Kronig, R. L. *Physica* **1939**, *6*, 33.

(23) (a) Orbach, R. *Proc. R. Soc. London, Ser. A* **1961**, *264*, 458. (b) Orbach, R. *Proc. R. Soc. London, Ser. A* **1961**, *264*, 458.